Permselective Graphene Oxide Membrane for Highly Stable and Anti-Self-Discharge Lithium–Sulfur Batteries

Jia-Qi Huang,[†,§] Ting-Zhou Zhuang,[†,§] Qiang Zhang,[*,†] Hong-Jie Peng,[†] Cheng-Meng Chen,[‡] and Fei Wei[†]

[†]Beijing Key Laboratory of Green Chemical Reaction Engineering and Technology, Department of Chemical Engineering, Tsinghua University, Beijing 100084, China and [‡]Key Laboratory of Carbon Materials, Institute of Coal Chemistry, Chinese Academy of Sciences, Taiyuan 030001, China. [§]J.-Q.H. and T.-Z.Z. contributed equally to this work.

ABSTRACT Lithium–sulfur batteries hold great promise for serving as next generation high energy density batteries. However, the shuttle of polysulfide induces rapid capacity degradation and poor cycling stability of lithium–sulfur cells. Herein, we proposed a unique lithium–sulfur battery configuration with an ultrathin graphene oxide (GO) membrane for high stability. The oxygen electronegative atoms modified GO into a polar plane, and the carboxyl groups acted as ion-hopping sites of positively charged species (Li^+) and rejected the transportation of negatively charged species (S_n^{2-}) due to the electrostatic interactions. Such electrostatic repulsion and physical inhibition largely decreased the transference of polysulfides across the GO membrane in the lithium–sulfur system. Consequently, the GO membrane with highly tunable functionalization properties, high mechanical strength, low electric conductivity, and facile fabrication procedure is an effective permselective separator system in lithium–sulfur batteries. By the incorporation of a permselective GO membrane, the cyclic capacity decay rate is also reduced from 0.49 to 0.23%/cycle. As the GO membrane blocks the diffusion of polysulfides through the membrane, it is also with advantages of anti-self-discharge properties.

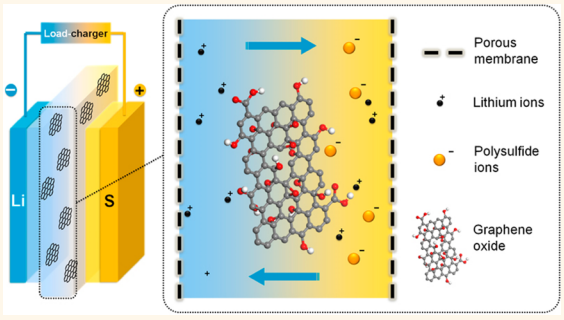

KEYWORDS: membrane · graphene oxide · lithium–sulfur battery · polysulfide

Electrochemical energy storage systems (*e.g.*, rechargeable batteries, flow batteries, fuel cells, and supercapacitors) have been widely used to store energy. An electrochemical energy storage system commonly includes electrodes, electrolytes, and separators. The exploration of novel materials as building blocks of electrodes in the system has been extensively investigated, and the energy density of the energy devices has been dramatically improved during the past several decades.[1−4] For instance, the great success of Li-ion batteries since the 1990s has flourished in portable devices and electrical vehicles. With the increasing demand for energy storage devices for future transportation, personal electrical devices, as well as controllable energy harvesting/storage from renewable energy sources, it is crucial to develop a rechargeable energy storage system with high energy density.

Sulfur is in vogue for promising multielectron transfer redox chemistry.[5−10] When the sulfur was employed as a counterpart for the lithium metal anode, the as-obtained lithium–sulfur batteries were with an unparalleled theoretical energy density of 2600 Wh kg^{-1}. The use of sulfur as the cathode materials exhibits rich advantages in environmental benignancy, natural abundance, low cost, and a wide operating temperature range. The redox pathway between the lithium metal anode and the elemental sulfur cathode can be described as

$$S_8 + Li^+ + e^- \rightarrow Li_2S_x (2.4 - 2.1\ V) \quad (1)$$

$$Li_2S_x + Li^+ + e^- \rightarrow Li_2S_2 \text{ and/or } Li_2S\ (2.1 - 1.5\ V) \quad (2)$$

* Address correspondence to zhang-qiang@mails.tsinghua.edu.cn.

Received for review December 16, 2014 and accepted February 16, 2015.

Published online February 16, 2015
10.1021/nn507178a

In organic electrolyte, soluble lithium polysulfides are generated in the sulfur cathode through reaction 1, and the polysulfides convert to insoluble lithium sulfide (Li_2S_2 and/or Li_2S) through eq 2 at the end of the discharge process. Such an electrochemical reaction includes a solid−liquid−solid phase transformation of the active sulfur materials, which induces severe complexity for highly reversible operations. Generally, the lithium−sulfur system is facing several drawbacks. First, the element sulfur and Li_2S/Li_2S_2 are highly insulating. Second, both the sulfur cathodes and lithium anodes suffer from large volume change during cycling. Third, polysulfide intermediates diffuse between cathode and anode sides and cause side reactions (so-called shuttle effect), which induces low Coulombic efficiency, unexpected self-discharge, and fast fading of capacity.

To solve these challenges for lithium−sulfur batteries, developing electrode materials *via* composite sulfur cathodes[11−20] and new electrolytes (*e.g.*, solid electrolyte,[21,22] lithium salt additive,[23,24] and polysulfide-containing electrolyte[25]) has been widely reported. The introduction of conductive porous frameworks can not only render the sulfur composite cathodes with high electronic conductivities and enough space for volume expansion but also restrain the diffusion of polysulfides by the confinement of polysulfides with hierarchical pores and/or strong coupled interfaces.[26] The incorporation of a polysulfide reservoir,[27,28] organic coating layer,[29,30] and carbon-based interlayer (*e.g.*, microporous carbon paper, graphene-based film)[31−35] for the sulfur cathode is also proven to be efficient to confine polysulfides within the cathode side. However, despite the progress in polysulfide entrapment, the rapid decay induced by polysulfides has not been fully addressed.

As an important component in battery systems, electrolyte/membrane systems contribute to the ionic connection between the cathode and anode, while the membranes serve as an electronic insulator to prevent the short circuit between the anode and cathode. Routine membranes in battery systems are normally porous polymers, which separate the two electrodes with no influence on the transportation of ions through the membrane.[36] Polysulfides generated in a lithium−sulfur system can also diffuse freely through the membranes and react with the metal lithium anode, which induces the degradation of the battery performance. Therefore, an ideal separator for lithium−sulfur batteries is expected to reduce reactivity of long-chain polysulfides with the metallic lithium and to homogeneously distribute the end-discharge products during cycling.[37] Cui and co-workers proposed a thin conductive coating on the separator to prevent the formation of the inactive sulfur-related species layer for lithium−sulfur batteries with significantly improved specific capacity and cycling stability.[38] By replacing the routine membrane system with ion-selective separators, the performance and safety of lithium-ion batteries was significantly improved.[39−43] A cationic selective Nafion membrane with $-SO_3^-$-coated channels allows ion hopping of positive charge species (Li^+) but rejects the transportation of anions (such as polysulfide anions (S_n^{2-}) in this specific case due to the electrostatic interactions). By the introduction of the Nafion membrane, the shuttle of polysulfides between the cathode and anode can be greatly suppressed.[41−43] However, the permeability of the Nafion membrane is relatively low, and a high loading amount of Nafion also influences the overall energy density of the lithium−sulfur cell. If a novel ion-selective but highly permeable membrane can be developed, the shuttle of polysulfides and self-discharge would be effectively retarded, and both the energy density and power density of lithium−sulfur batteries can therefore be fully demonstrated.

Graphene, a typical two-dimensional material, has been mostly known for its excellent intrinsic properties. As one of the most attractive macroscopic forms of graphene-based materials, graphene oxide (GO) membranes are inherently of good mechanical strength and may stand on its own.[44−46] Recently, Geim and co-workers have found that the GO membrane allows unimpeded permeation of water and rapid diffusion of smaller ions through the membranes.[47,48] The GO is also reported to serve as a proton exchange membrane after ozone treatment[49] or an ion-selective membrane for alkali and alkaline earth cations.[50,51]

Based on these considerations, the GO membrane with negative charges is expected to be permeable for lithium ions but reject anions. Hence, it is a promising permselective separator for lithium−sulfur batteries. Compared to conductive carbon interlayers that serve as an additional carbon scaffold and mainly as a physical barrier,[31−35] GO membranes are able to block polysulfide by electrostatic repulsion and steric exclusion, which are more efficient in long-term inhabitation of the shuttle effect. On the other hand, the typical 2D structure of a GO flake can reduce the loading amount to form an effective polysulfide shield layer compared to reported polymer coating layers.[41]

In this contribution, we demonstrated that the GO membrane exhibited high permselectivity to lithium ions and afforded lithium−sulfur batteries with extraordinary stability and an anti-self-discharge feature. As shown in Figure 1, when a cationic permselective GO membrane was applied in lithium−sulfur batteries, the anions of polysulfides were expected to be confined on the cathode side. The shuttle of polysulfides between the cathode and anode sides can thereby be significantly suppressed. Meanwhile, the lithium cations can easily transport through the cationic permselective GO membrane, which guaranteed the high capacity and

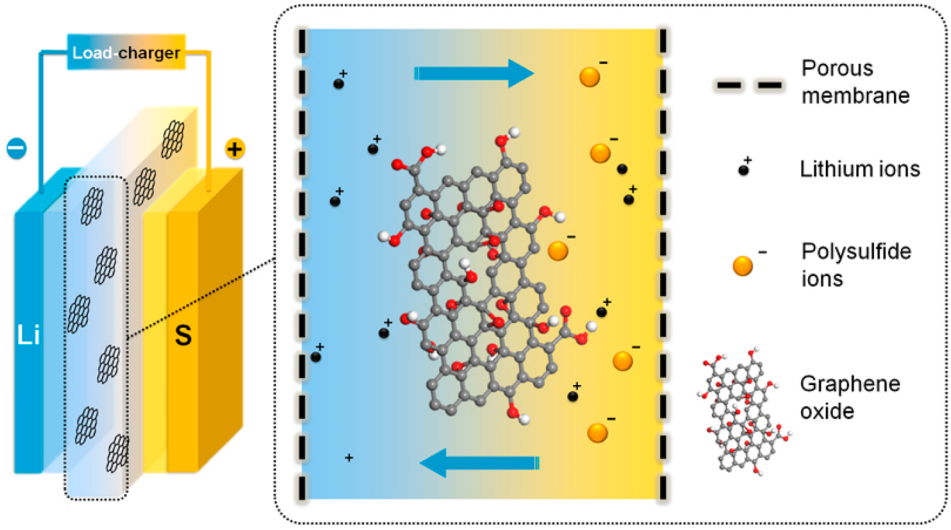

Figure 1. Schematic of a GO membrane incorporates a lithium−sulfur battery. GO membrane was sandwiched between cathode and anode electrodes, which may efficiently prohibit the shuttle of polysulfides through the membrane.

good rate performance of a lithium−sulfur cell. This ultrathin GO separator also offered remarkable improvement in the cyclic stability and self-discharging inhibition of lithium−sulfur batteries. This is also a prototype to demonstrate the potential application of GO-based membranes for advanced energy storage devices.

RESULTS AND DISCUSSION

Morphologies of GO Membranes. The GO mass produced by a modified Hummers' method[52] was employed as the building block to construct a GO membrane. With abundant oxygenated functional groups (mostly ether, hydroxyl, and carboxyl groups) on its basal plane, GO flakes were highly dispersible and wettable in polar solvents (such as water, ethanol, and 1,3-dioxolane (DOL)/1,2-dimethoxyethane (DME) mixture (v/v = 1/1), as indicated in the inset of Figure 2a). A high atomic oxygen content of 33% was determined by X-ray photoelectron spectroscopy (XPS) analysis of the GO membrane (Figure 2a). The oxygen-containing groups were assigned into five components: a peak at 530.5 eV for highly conjugated forms of carbonyl oxygen, such as quinone groups; a peak at 531.2 eV for carboxyl groups (CO(O)); a peak at 531.9 eV for nonaromatic carbonyl groups (C═O); a peak at 532.7 eV for ether-like groups (C−O); and a peak at 533.5 eV for oxygen in hydroxyl groups. Among the oxygen-containing functional groups, the oxygen atoms in carbonyl groups and ether-like groups accounted for 63 and 15%, respectively. These oxygen electronegative atoms modified the GO flake into a polar plane, and the carboxyl groups acted as ion-hopping sites of positively charged species (Li^+) and rejected the transportation of negatively charged species (S_n^{2-}) due to the electrostatic interactions. These functional groups and corrugated surface also prevented the GO flakes from dense stacking, which may significantly reduce the diffusion of lithium ions through the GO membrane.

Since the GO materials were highly dispersible in solvents, it can be easily processed into ultrathin membranes with facile vacuum filtration techniques. A vacuum filtration process was applied in this contribution to attach a membrane on a routine polymer separator. According to the scanning electron microscopy (SEM) image, the routine Celgard 2400 polypropylene (PP) separators have abundant pore structure of around 100 nm (Supporting Information Figure S1). With the coating of an ultrathin GO membrane at a low areal loading amount of 0.12 mg cm^{-2}, the pores are completely blocked by the adhesive GO flakes (Figure 2b). Besides, no GO flake penetrated into/through the pores distributed on the polymer separator. The GO membrane is composed of loosely but orderly stacked GO flakes from the cross section view (Figure 2c). The tunnels and corrugation between the GO flake laminates served as the channels for rapid transportation of lithium ions. The electrostatic repulsion and physical inhibition can largely decrease the transference of polysulfides across the GO membrane, serving as the separator in the lithium−sulfur system, while only slightly increasing the transportation resistance for lithium ions through the zigzag pathways between GO flakes.

Permeability of GO Membranes. The permeation properties of the as-fabricated membrane played a key role when the GO membrane was applied as a separator in a lithium−sulfur cell. A visualized cell was set up to evidently demonstrate the role of the GO membrane in prohibiting the diffusion of polysulfide anions that originated in the shuttle effect in lithium−sulfur batteries (Figure 3). An H-type glass cell was employed to hold the DOL/DME solvent without polysulfide in the

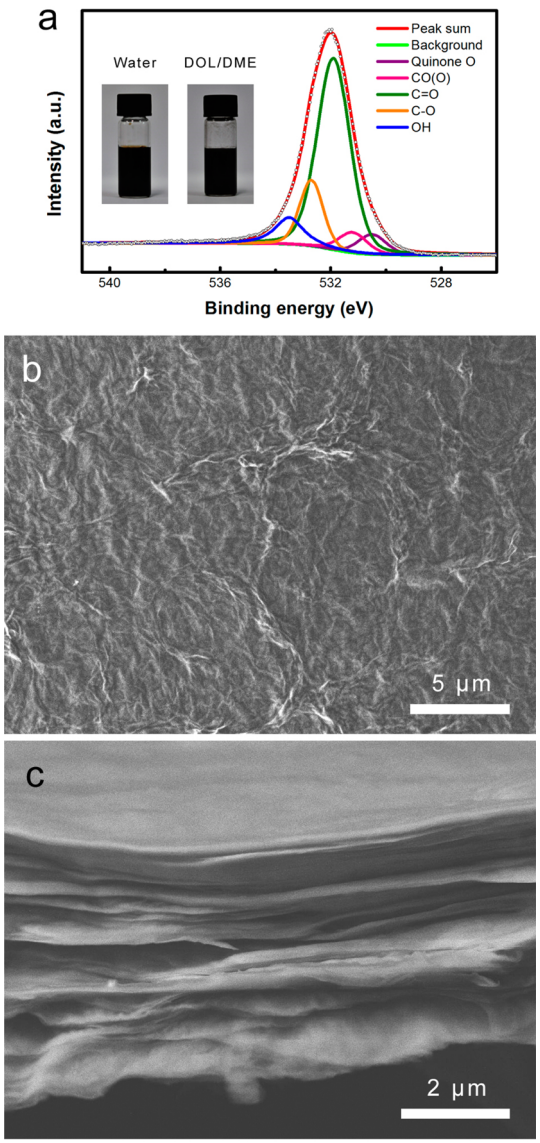

Figure 2. Structure of GO membranes. (a) Fitting results of O 1s XPS spectra of GO materials (insets are the digital photographs of GO flakes dispersed in water and DOL/DME); SEM images: (b) bird view and (c) cross section of the GO membrane.

right chamber and solvent with 0.5 M Li_2S_7 in the left chamber, in which the two chambers were separated by a routine membrane or a GO membrane. In the case of cells with a routine PP membrane (Figure 3, inset top line), polysulfides diffused through the separator and the right chamber turned from colorless to dark brown within 8.0 h. The gray level ascended to a high level in the right chamber. It can be speculated that polysulfides can easily diffuse across the membrane and reached the lithium metal side, in which case a severe shuttle effect was inevitable in a lithium−sulfur cell with a routine membrane. In contrast, the diffusion of polysulfides can be significantly suppressed with an ultrathin GO membrane (Figure 3, inset bottom line). The right chamber stayed colorless even after 16.0 h. To further characterize the distribution of sulfur-containing

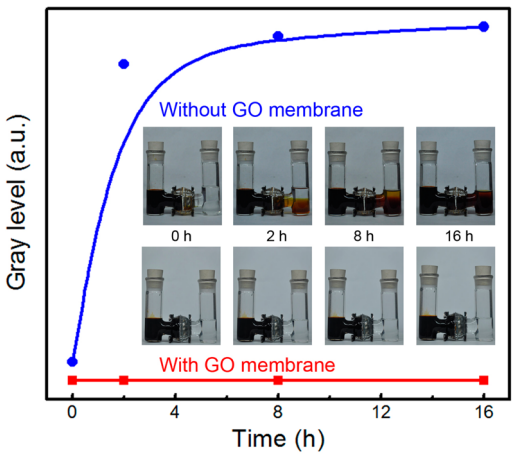

Figure 3. Permselectivity of the GO membrane. Optical images of the diffusion of high-order polysulfides: H-type cell without a GO membrane (inset top), H-type cell with a GO membrane (inset bottom), and the dependence of the gray level in the right chamber as diffusion duration.

species in the GO membrane, the depth profile of sulfur element distribution after the electrochemical charge/discharge cycles was analyzed by Auger electron spectroscopy (Figure S2). The depth profile indicated that the polysulfides are blocked within a top thin GO layer (5−15 nm in thickness). Considering that the polysulfides are a mixture of long-chain and short-chain polysulfides, we expected the GO membrane to block the transportation of both short-chain and long-chain polysulfides from Li_2S_4 to Li_2S_8.

The change of lithium-ion transference number with GO membrane was determined to quantitatively describe the contribution of lithium ions in charge transfer through the membranes. The lithium-ion transference number was measured by a potentiostatic polarization method in a coin cell.[53] To exclude the influence of electrochemical contact on the performance of the GO membrane, this work was conducted in a sandwich configuration with the GO membrane stacked between two routine separators. With a small constant potential of 10 mV applied in a symmetric coin cell with lithium foils as two electrodes, an $i-t$ curve with a decrease of initial current to the steady-state value was obtained. During this process, the anion current vanished in the steady state, and thus the cation transference number can be determined. The transference numbers in the cell with polysulfide/DOL/DME electrolyte were tested (Figure S3). Significant improvement from 0.40 to 0.93 can be observed by incorporating the GO membrane into this system. Apparently, the GO membrane was very efficient for blocking the diffusion of polysulfide anions. The permeability of GO membranes for lithium ions is also well-known for its performance in lithium−sulfur cells, especially for excellent rate capability. The lithium-ion diffusion coefficient was evaluated by a series of cyclic voltammograms (CVs) with different scan rates and

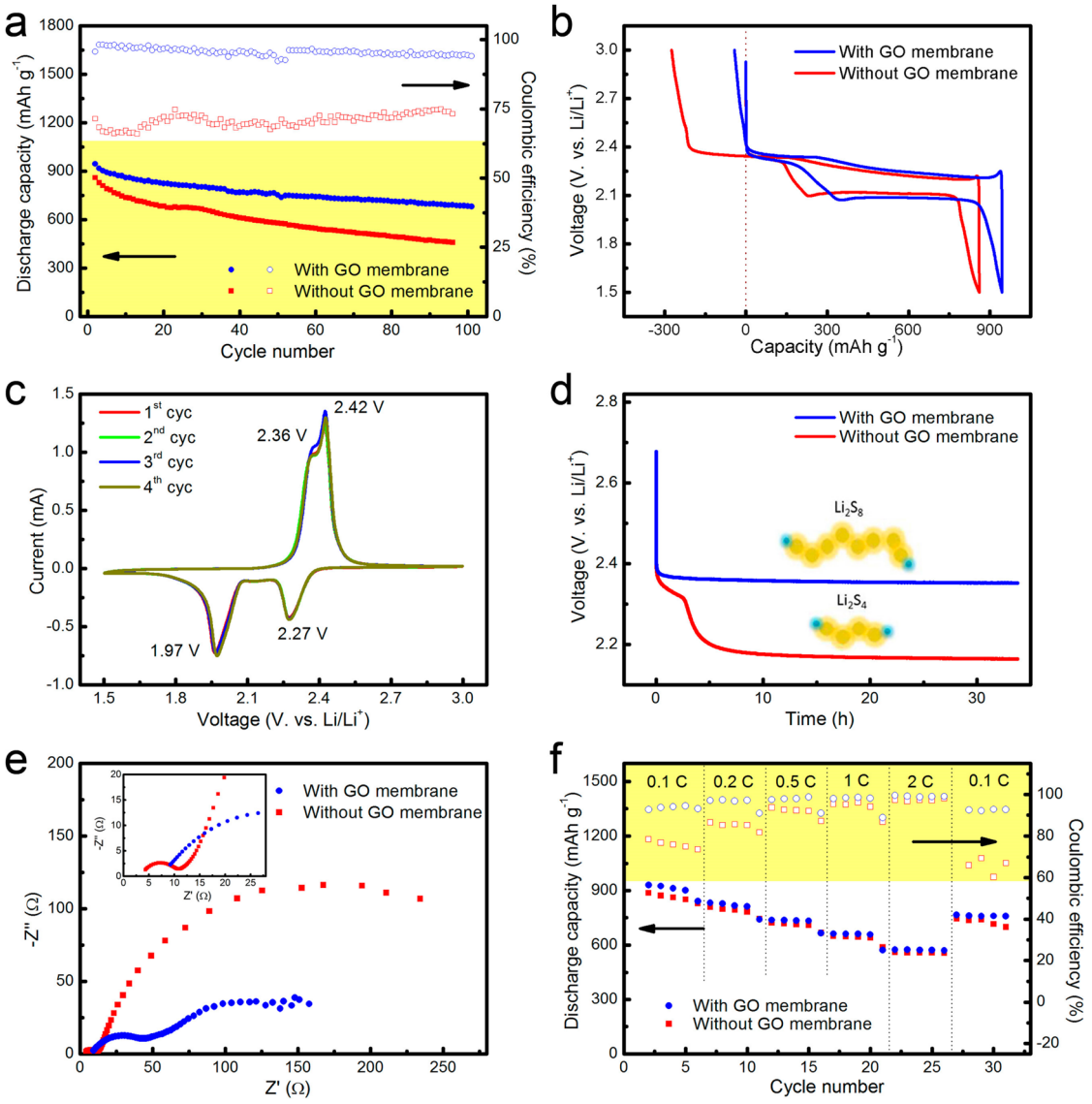

Figure 4. Electrochemical performance of the GO-membrane-incorporated lithium−sulfur batteries. (a) Cycling performance at a rate of 0.1 C with/without a GO membrane; (b) galvanostatic charge−discharge profiles at a rate of 0.1 C; (c) CV profiles with a GO membrane at a scan rate of 0.1 mV s^{-1}; (d) open circuit voltage profiles showing the self-discharge behavior; (e) electrochemical impedance spectra (inset is the enlarged EIS at the high-frequency region); and (f) rate performance of lithium−sulfur batteries with/without a GO membrane.

was calculated by the Randles−Sevick equation.[54,55] In the CVs of the lithium−sulfur system, we assigned the anodic peak at around 2.5 V and the cathodic peaks at around 2.0 and 2.3 V as peaks A, B, and C, respectively. As plotted in Figure S4a,b and the linear fit in Figure S4c, the linear fitting of the peak current was highly relevant, indicating a diffusion-controlled process. The diffusion coefficients at different CV voltage regions were determined to be D_{Li}^{+}(A1) = 2.26 × 10^{-8} cm^2 s^{-1}, D_{Li}^{+}(B1) = 9.07 × 10^{-9} cm^2 s^{-1}, and D_{Li}^{+}(C1) = 9.00 × 10^{-9} cm^2 s^{-1} for cells of the routine membrane. After the incorporation of the GO membrane, the diffusion coefficients became D_{Li}^{+}(A2) = 3.18 × 10^{-8} cm^2 s^{-1}, D_{Li}^{+}(B2) = 5.38 × 10^{-9} cm^2 s^{-1}, and D_{Li}^{+}(C2) = 7.67 × 10^{-9} cm^2 s^{-1}. The average values of D_{Li}^{+} indicated that the introduction of GO did not notably degrade the diffusion of the lithium ion. In general, GO membranes are highly permselective to lithium ions against polysulfide anions, while the incorporation of GO membranes leaves only a slight impact on the transfer of lithium ions across the separator.

Electrochemical Performances. GO membrane systems were also integrated into lithium−sulfur batteries to explore its role on the electrochemical performance. As shown in Figure 4a, the Coulombic efficiency of the lithium−sulfur cell without a GO membrane was 67−75% in 100 cycles. In contrast, the batteries with a GO membrane (loading amount of 0.12 mg cm^{-2}) kept a very high Coulombic efficiency of 95−98% in 100 cycles at 0.1 C. With the incorporation of the GO membrane, the shuttle factor that reflects the degree of shuttle effect was reduced from 0.81 to 0.06. Note

that no $LiNO_3$ or other additive was introduced into the electrolyte to protect the anode electrode, and a lithium−sulfur cell at a very low charge/discharge current density of 0.1 C was common with a severe shuttle effect and low Coulombic efficiency of less than 70−90% for common carbon/sulfur composite cathodes (shuttle factor was normally larger than 0.3−0.77).[12,56,57] The use of the GO membrane was of great significance in improving the Coulombic efficiency of the cell, indicating the suppressed shuttle effect in the cell. Moreover, as the GO membrane hindered the chemical reactions between metallic lithium and high-order polysulfides, the active material loss was reduced and the discharge capacity increased accordingly. Therefore, a slightly higher initial discharge capacity of 920 mAh g^{-1} was obtained on the cell with a GO separator, over the value of 860 mAh g^{-1} on the cell without a GO membrane. Furthermore, the cyclic capacity decay rate was reduced from 0.49 to 0.23%/cycle, showing a higher cyclic stability for the cell with a GO membrane. When we mounted a GO membrane of a large areal density of 0.24 mg cm^{-2}, a high Coulombic efficiency of *ca.* 97% was achieved. However, the cyclic capability degraded, which may be related to the elevated resistance induced by the thick GO membrane (Figure S5a). The effect of the GO membrane on the electrochemical performance of Li−S cells was also verified on a sulfur cathode based on carbon black (Figure S6). The incorporation of the GO membrane leads to an improved initial discharge capacity from 855 to 1040 mAh g^{-1} and an increased Coulombic efficiency from *ca.* 70% to greater than 92%. These results indicated that the GO membrane is one versatile system for different sulfur cathodes in high-performance lithium−sulfur cells. Compared with other carbon material sandwiched layers (including multiwalled carbon nanotubes, SuperP, and Ketjen black at same loading amount), the GO membrane exhibited a remarkable advantage in improving the Coulombic efficiency of Li−S cells (Figure S7), which can be attributed to the electrostatic repulsion and steric exclusion effect of GO on polysulfides.

The overcharge behaviors of lithium−sulfur cells with/without a GO membrane were investigated by the galvanostatic charge−discharge profiles (Figure 4b). Without a GO membrane, severe overcharge can be observed. However, the overcharge phenomenon in the cell with the GO membrane was greatly reduced. The detailed electrochemical behavior was further probed by the CV (Figure 4c). Two typical peaks were determined during the cathodic scan, corresponding to the reduction process that occurs in two stages: a peak at 2.27 V for the reduction of cyclo-S_8 to high-order lithium polysulfides (Li_2S_x; $x = 4-8$); and peak at 1.97 V for the further reduction to lithium sulfides (Li_2S or Li_2S_2). In the subsequent anodic scan, the two peaks observed at 2.36 and 2.42 V were assigned to the formation of Li_2S_n ($n > 2$) and cyclo-S_8, respectively. The nearly overlapped peak position can be assigned to the high reversibility endowed by GO membranes.

The severe self-discharge is another major drawback of lithium−sulfur batteries induced by the shuttle effect. In most cases, around 30% of the capacity self-discharges within several hours,[58−60] which is not acceptable for a practical electrochemical device. In this work, the open circuit voltages of lithium−sulfur cells were monitored to describe how the GO membrane contributed to the anti-self-discharge feature. It was observed that the open circuit voltage of a normal cell only with a routine membrane decays drastically in 5.0 h (Figure 4d). The capacity contributed by the high plateau of sulfur discharge vanished in 4.0 h, which indicated the spontaneous reduction of high-order polysulfides into low-order polysulfides. This self-discharging was significantly inhibited by the incorporation of the GO membrane, in which case the open circuit voltage remained at 2.5 V for more than 30 h due to the prohibition of high-order polysulfide diffusion. This result is in accordance with the discharge capacity after resting (Figure S8). For a cell with a GO membrane, a high retention of 93.3% after one 24 h rest can be preserved, in which the high plateau is maintained, as well. In contrast, severe self-discharge behavior was observed for the cell without a GO membrane. The capacity retention dropped to 60.7% after a 24 h rest, and the high plateau was almost eliminated due to conversion of high-order polysulfides into low-order ones during the self-discharging process.

The role of the GO membrane in a lithium−sulfur cell was further probed by the electrochemical impedance spectra (EIS) (Figure 4e). Both the EIS for a cell without and with a GO membrane presented two typical semicircles corresponding to the resistances for ion transportation in the high-frequency region (R_f) and resistance for charge transfer in the medium-frequency region (R_{ct}).[61] Compared to the EIS of a cell with routine membranes, the lithium−sulfur cell with a GO membrane showed an EIS with enlarged R_f and reduced R_{ct}. These phenomena were attributed to the additional resistance in ion transportation by the GO membrane and also the reduced charge transfer resistance through the solid electrolyte interphase by inhibiting the formation of lithium sulfide layers on metallic lithium. Although the introduction of a GO membrane caused the slight increase of lithium-ion transfer resistance, the lithium-ion diffusion coefficient and ion conductivity still indicated a highly efficient lithium-ion transport with the GO membrane, and the lithium−sulfur cell with a GO membrane can still offer excellent rate performance (Figure 4f). With the current densities varied between 0.2 and 2.0 C, the discharge capacities of the cell with a GO membrane exhibited a trend similar to that of conventional cells with a capacity retention of 63%. When the charge/discharge

current reduced back to 0.2 C, a higher discharge capacity of 765 mAh g^{-1} was recovered for the cell with a GO membrane (725 mAh g^{-1} for the cell without a GO membrane). The Coulombic efficiencies of cells with a GO membrane between 93 and 99.5% were superior to that of the cells with routine polymer separators (Coulombic efficiency between 60 and 95%). If a thick GO separator with an areal loading of 0.24 mg cm^{-2} was employed, although high Coulombic efficiency of 95% could be achieved, the capacity retention at high current density of 2.0 C was reduced to 21% due to the higher polarization (Figure S5c,d). Instead, if a thin GO membrane with an areal loading of 0.03 mg cm^{-2} was used, no significant improvement in the Coulombic efficiency was observed, indicating the low impact on polysulfide blocking (Figure S5c,d). This indicated that the high permeability of lithium ions and the high blocking efficiency of polysulfides were achieved with a GO membrane of proper thickness.

The success of an ultrathin GO membrane exhibiting high permselectivity to lithium ions and affording a lithium−sulfur battery with extraordinary stability and an anti-self-discharge feature was attributed from the following reasons: (1) In view of the structure of GO, it can be considered as numerous small sp^2 clusters decorated asymmetrically on the sp^3 C−O matrix.[44−46] When a large amount of GO flakes are stacked together to form the GO laminates, the sp^2 clusters will connect together across all stacking layers to form a sp^2 nanocapillary network, which provides selective pathways for small cations (*e.g.*, H^+,[49,62] Li^+, K^+,[47] Mg^{2+},[47] *etc.*) and served as a rapid Li^+ connection pathway between cathode and anode electrodes for excellent rate capability. (2) The GO membrane can suppress the diffusion of anions of polysulfides by electrostatic repulsion and steric exclusion, thus retarding the shuttle, improving the Coulombic efficiency, and inhibiting the self-discharge of the cell.

CONCLUSIONS

GO membranes with highly tunable functionalization properties, high mechanical strength, low electric conductivity, and facile fabrication procedures were effective permselective separator systems in lithium batteries. With the incorporation of a permselective GO membrane, the lithium−sulfur batteries afforded an improved Coulombic efficiency from 67−75% to over 95−98% at 0.1 C. The cyclic capacity decay rate was also reduced from 0.49 to 0.23%/cycle. As the GO membrane blocks the diffusion of polysulfides through the membrane, it was also with advantages of anti-self-discharging properties. Compared to the fast open circuit voltage drop of cells with a routine membrane within 5.0 h, the cell with GO membrane presented a stable open circuit voltage after 30 h. The permselectivity of lithium ions over polysulfide anions resulted from both the physical barrier effect and the chemical barrier effect with oxygenated functional groups on the GO flakes. We expect GO membranes to be highly attractive for enhancing the performance of lithium−sulfur batteries. In addition, this work also offers a general strategy to combine the GO membrane with a rechargeable battery, which is crucial for illustrating the potential of a functional membrane for advanced energy storage and understanding the dynamic changes on the electrode. This approach may also provide a novel cell configuration applicable in supercapacitors, lithium-ion batteries, lithium−air batteries, and fuel cells, which requires delicate control of ion transportations for high-performance devices.

EXPERIMENTAL SECTION

Membrane Preparation. GO was prepared by a modified Hummers' method. The as-obtained GO was dried at 90 °C for 6.0 h and then dissolved in DOL/DME (v/v = 1:1) electrolyte under ultrasonication for 1.0 h. The as-prepared GO solution was then filtered through conventional Celgard 2400 separators to obtain a GO membrane on routine separators with an areal loading of 0.03−0.24 mg cm^{-2}. The typical GO membrane applied in this work is 0.12 mg cm^{-2}.

Membrane Characterizations. The morphology of the GO membrane was examined by a JSM 7401F (JEOL Ltd., Japan) SEM operated at 5.0 kV. The XPS spectra were obtained on an Escalab 250Xi. The visualized diffusion test was carried out in an H-type cell to examine the properties of the GO interlayer. The control test was carried out by using a routine membrane in the middle without GO. The left chamber was filled with 0.50 M Li_2S_7 solution with DOL/DME (v/v = 1:1) as the solvent, while the right chamber was only filled with DOL/DME solvent (v/v = 1:1). The Li_2S_7 was prepared by a synproportionation reaction between Li_2S and S with a mole ratio of 1:6.

The transfer number of the lithium ion was measured with a potentiostatic polarization method in a symmetrical 2025 cell configuration with lithium metal as two counter electrodes, 0.5 M Li_2S_7 solution with DOL/DME (v/v = 1:1) as electrolyte, and GO membrane or Celgard 2400 as the separator. The test involved a potentiostatic polarization process with the constant potential at 10 mV for 1.0 h to determine the initial current (I_0) and steady-state current (I_{ss}), and two EIS tests right before and after the potentiostatic polarization process to calculate the electrode resistances (R_0 for initial resistance and R_{ss} for steady-state resistance). The transfer number for the cation is given by

$$t_+ = \frac{I_{ss}(\Delta V - I_0 R_0)}{I_0(\Delta V - I_{ss} R_{ss})} \quad (3)$$

Lithium-ion diffusion coefficient D_{Li}^+ (cm^2 s^{-1}) is evaluated by cyclic voltammetry and calculated according to the Randles−Sevick equation:

$$I_p = 2.69 \times 10^5 n^{1.5} A D_{Li^+}^{0.5} C_{Li} v^{0.5} \quad (4)$$

in which I_p (A) is the peak current, n represents the number of electrons of in the reaction (for Li−S batteries, n = 2), A (cm^2) indicates the electrode area (1.327 cm^2 here), C_{Li}^+ (mol mL^{-1}) means the lithium-ion concentration in the electrolyte, and v stands for the scanning rate (V s^{-1}).

The CVs at different scanning rates are given as Figure S4a,b. To calculate D_{Li}^+, the peak current values in CV and the square root of the scan rate ($v^{0.5}$) are linear fitted as Figure S4c.

We calculated the diffusion coefficients at one anodic stage (2.4−2.5 V) and two cathodic stages (2.0−2.1 and 2.2−2.3 V).

The distribution of sulfur in the GO membrane after five 0.2 C charge/discharge cycles is also characterized semiquantitatively by Auger electron spectroscopy equipped with an Ar-ion sputter (AES, PHI 700) with a sputter rate of 21 nm min^{-1} for SiO_2.

Calculation of Shuttle Factor. As suggested by Mikhaylik and Akridge,[58] the shuttle effect is considered as the competition between the reactions induced by the charge/discharge current and by the diffusion of polysulfides (side reaction). Consequently, a shuttle factor is defined to reflect the extent of shuttle effect. The shuttle factor is expressed as

$$f = k_s \cdot q_H \cdot [S_{total}]/I \quad (5)$$

where k_s is the heterogeneous reaction constant related to polysulfide diffusion and reaction, q_H is the theoretical specific charge/discharge capacities of the high plateau, and I is the charge/discharge current.

The relationship between the Coulombic efficiency and the shuttle factor is expressed as formula 6:[58,63]

$$C_{eff} = \frac{Q_{DH} + Q_{DL}}{Q_{CH} + Q_{CL}} = \frac{2f + \ln(1+f)}{2f - \ln(1-f)} \quad (6)$$

Electrochemical Performance Tests. Standard 2025 coin cells were used to evaluate the electrochemical performance of the GO-membrane-incorporated lithium−sulfur batteries. The cathode slurry was prepared by mixing 63 wt % sulfur, 27 wt % carbon nanotubes, and 10% poly(vinylidene fluoride) binder in *N*-methylpyrrolidone (NMP) solvent dispersant. In the case of carbon black as the conducting agent, composition was 63 wt % sulfur, 27 wt % carbon black, and 10 wt % binder in NMP. The cathode with an areal sulfur loading of 1.0−1.5 mg cm^{-2} was constructed by coating the slurry on aluminum foil and drying at 60 °C for 24.0 h. The metallic lithium disk was used as the anode. Then 1.0 mol L^{-1} LiTFSI solution in DOL/DME (v/v = 1:1) was used for the cells. The membranes used in the cell were two routine Celgard 2400 membranes, or GO-membrane-sandwiched Celgard membranes. Thirty microliter of electrolyte was added between two Celgard membranes to confirm the wetting of the GO membranes. The coin cells were tested in galvanostatic mode at various currents within a voltage range of 1.5−3.0 V using Neware multichannel battery cyclers. Both CV and EIS were performed on a Solartron 1470E electrochemical workstation. The CV was scanned at a rate of 0.10 mV s^{-1}. The capacities were calculated based on the mass of sulfur in the cathodes.

Conflict of Interest: The authors declare no competing financial interest.

Acknowledgment. This work was supported by the National Natural Science Foundation of China (21306103 and 21422604) and the Key Laboratory of Carbon Materials (KLCMKFJJ1405). The authors thank Peng-Zhan Sun for helpful discussions.

Supporting Information Available: The morphology of a routine separator, potentiostatic polarization of Li−S cell, cyclic voltammogram results, Auger electron spectroscopy results for cycled GO membrane, self-discharge tests, and electrochemical performance of the cell with different GO membranes, different nanocarbon interlayers, and different cathode electrodes. This material is available free of charge *via* the Internet at http://pubs.acs.org.

REFERENCES AND NOTES

1. Liu, C.; Li, F.; Ma, L. P.; Cheng, H. M. Advanced Materials for Energy Storage. *Adv. Mater.* **2010**, *22*, E28–E62.
2. Nishihara, H.; Kyotani, T. Templated Nanocarbons for Energy Storage. *Adv. Mater.* **2012**, *24*, 4473–4498.
3. Maiti, U. N.; Lee, W. J.; Lee, J. M.; Oh, Y.; Kim, J. Y.; Kim, J. E.; Shim, J.; Han, T. H.; Kim, S. O. 25th Anniversary Article: Chemically Modified/Doped Carbon Nanotubes & Graphene for Optimized Nanostructures & Nanodevices. *Adv. Mater.* **2014**, *26*, 40–67.
4. Xie, K. Y.; Wei, B. Q. Materials and Structures for Stretchable Energy Storage and Conversion Devices. *Adv. Mater.* **2014**, *26*, 3592–3617.
5. Manthiram, A.; Fu, Y.; Chung, S. H.; Zu, C. X.; Su, Y. S. Rechargeable Lithium−Sulfur Batteries. *Chem. Rev.* **2014**, *114*, 11751–11787.
6. Nazar, L. F.; Cuisinier, M.; Pang, Q. Lithium−Sulfur Batteries. *MRS Bull.* **2014**, *39*, 436–442.
7. Bresser, D.; Passerini, S.; Scrosati, B. Recent Progress and Remaining Challenges in Sulfur-Based Lithium Secondary Batteries—A Review. *Chem. Commun.* **2013**, *49*, 10545–10562.
8. Xu, G. Y.; Ding, B.; Pan, J.; Nie, P.; Shen, L. F.; Zhang, X. G. High Performance Lithium−Sulfur Batteries: Advances and Challenges. *J. Mater. Chem. A* **2014**, *2*, 12662–12676.
9. Yin, Y. X.; Xin, S.; Guo, Y. G.; Wan, L. J. Lithium−Sulfur Batteries: Electrochemistry, Materials, and Prospects. *Angew. Chem., Int. Ed.* **2013**, *52*, 13186–13200.
10. Zhang, S. S. Liquid Electrolyte Lithium/Sulfur Battery: Fundamental Chemistry, Problems, and Solutions. *J. Power Sources* **2013**, *231*, 153–162.
11. Ji, X. L.; Lee, K. T.; Nazar, L. F. A Highly Ordered Nanostructured Carbon−Sulphur Cathode for Lithium−Sulphur Batteries. *Nat. Mater.* **2009**, *8*, 500–506.
12. Wang, H. L.; Yang, Y.; Liang, Y. Y.; Robinson, J. T.; Li, Y. G.; Jackson, A.; Cui, Y.; Dai, H. J. Graphene-Wrapped Sulfur Particles as a Rechargeable Lithium−Sulfur Battery Cathode Material with High Capacity and Cycling Stability. *Nano Lett.* **2011**, *11*, 2644–2647.
13. Huang, H. B.; Song, Z. G.; Wei, N.; Shi, L.; Mao, Y. Y.; Ying, Y. L.; Sun, L. W.; Xu, Z. P.; Peng, X. S. Ultrafast Viscous Water Flow through Nanostrand-Channelled Graphene Oxide Membranes. *Nat. Commun.* **2013**, *4*, 2979.
14. Yang, Y.; Zheng, G. Y.; Cui, Y. Nanostructured Sulfur Cathodes. *Chem. Soc. Rev.* **2013**, *42*, 3018–3032.
15. Wang, D. W.; Zeng, Q. C.; Zhou, G. M.; Yin, L. C.; Li, F.; Cheng, H. M.; Gentle, I.; Lu, G. Q. Carbon/Sulfur Composites for Li−S Batteries: Status and Prospects. *J. Mater. Chem. A* **2013**, *1*, 9382–9394.
16. Song, J. X.; Xu, T.; Gordin, M. L.; Zhu, P. Y.; Lv, D. P.; Jiang, Y. B.; Chen, Y. S.; Duan, Y. H.; Wang, D. H. Nitrogen-Doped Mesoporous Carbon Promoted Chemical Adsorption of Sulfur and Fabrication of High-Areal-Capacity Sulfur Cathode with Exceptional Cycling Stability for Lithium−Sulfur Batteries. *Adv. Funct. Mater.* **2014**, *24*, 1243–1250.
17. Wang, L. N.; Zhao, Y.; Thomas, M. L.; Byon, H. R. *In Situ* Synthesis of Bipyramidal Sulfur with 3D Carbon Nanotube Framework for Lithium−Sulfur Batteries. *Adv. Funct. Mater.* **2014**, *24*, 2248–2252.
18. Zhao, M. Q.; Zhang, Q.; Huang, J. Q.; Tian, G. L.; Nie, J. Q.; Peng, H. J.; Wei, F. Unstacked Double-Layer Templated Graphene for High-Rate Lithium−Sulphur Batteries. *Nat. Commun.* **2014**, *5*, 3410.
19. Zhou, G. M.; Yin, L. C.; Wang, D. W.; Li, L.; Pei, S. F.; Gentle, I. R.; Li, F.; Cheng, H. M. Fibrous Hybrid of Graphene and Sulfur Nanocrystals for High-Performance Lithium−Sulfur Batteries. *ACS Nano* **2013**, *7*, 5367–5375.
20. Rong, J. P.; Ge, M. Y.; Fang, X.; Zhou, C. W. Solution Ionic Strength Engineering as a Generic Strategy To Coat Graphene Oxide (GO) on Various Functional Particles and Its Application in High-Performance Lithium−Sulfur (Li−S) Batteries. *Nano Lett.* **2014**, *14*, 473–479.
21. Lin, Z.; Liu, Z. C.; Fu, W. J.; Dudney, N. J.; Liang, C. D. Lithium Polysulfidophosphates: A Family of Lithium-Conducting Sulfur-Rich Compounds for Lithium−Sulfur Batteries. *Angew. Chem., Int. Ed.* **2013**, *52*, 7460–7463.
22. Lin, Z.; Liu, Z. C.; Fu, W. J.; Dudney, N. J.; Liang, C. D. Phosphorous Pentasulfide as a Novel Additive for High-Performance Lithium−Sulfur Batteries. *Adv. Funct. Mater.* **2013**, *23*, 1064–1069.
23. Suo, L. M.; Hu, Y. S.; Li, H.; Armand, M.; Chen, L. Q. A New Class of Solvent-in-Salt Electrolyte for High-Energy Rechargeable Metallic Lithium Batteries. *Nat. Commun.* **2013**, *4*, 1481.
24. Barghamadi, M.; Best, A. S.; Bhatt, A.; Hollenkamp, A. F.; Musameh, M. M.; Rees, R.; Ruether, T. Lithium−Sulfur

Batteries: The Solution Is in the Electrolyte, but Is the Electrolyte a Solution? *Energy Environ. Sci.* **2014**, *7*, 3902–3920.
25. Chen, S. R.; Dai, F.; Gordin, M. L.; Wang, D. H. Exceptional Electrochemical Performance of Rechargeable Li–S Batteries with a Polysulfide-Containing Electrolyte. *RSC Adv.* **2013**, *3*, 3540–3543.
26. Peng, H. J.; Hou, T. Z.; Zhang, Q.; Huang, J. Q.; Cheng, X. B.; Guo, M. Q.; Yuan, Z.; He, L. Y.; Wei, F. Strongly Coupled Interfaces between Heterogeneous Carbon Host and Sulfur-Containing Guest for Highly-Stable Lithium–Sulfur Batteries: Mechanistic Insight into Capacity Degradation. *Adv. Mater. Interfaces* **2014**, *1*, 1400227.
27. Yao, H. B.; Zheng, G. Y.; Hsu, P. C.; Kong, D. S.; Cha, J. J.; Li, W. Y.; Seh, Z. W.; McDowell, M. T.; Yan, K.; Liang, Z.; Narasimhan, V. K.; Cui, Y. Improving Lithium–Sulphur Batteries through Spatial Control of Sulphur Species Deposition on a Hybrid Electrode Surface. *Nat. Commun.* **2014**, *5*, 3943.
28. Ji, X.; Evers, S.; Black, R.; Nazar, L. F. Stabilizing Lithium–Sulphur Cathodes Using Polysulphide Reservoirs. *Nat. Commun.* **2011**, *2*, 325.
29. Yang, Y.; Yu, G. H.; Cha, J. J.; Wu, H.; Vosgueritchian, M.; Yao, Y.; Bao, Z. A.; Cui, Y. Improving the Performance of Lithium–Sulfur Batteries by Conductive Polymer Coating. *ACS Nano* **2011**, *5*, 9187–9193.
30. Wang, J. L.; Yao, Z. D.; Monroe, C. W.; Yang, J.; Nuli, Y. N. Carbonyl-β-Cyclodextrin as a Novel Binder for Sulfur Composite Cathodes in Rechargeable Lithium Batteries. *Adv. Funct. Mater.* **2013**, *23*, 1194–1201.
31. Su, Y. S.; Manthiram, A. Lithium–Sulphur Batteries with a Microporous Carbon Paper as a Bifunctional Interlayer. *Nat. Commun.* **2012**, *3*, 1166.
32. Zhou, G.; Pei, S.; Li, L.; Wang, D. W.; Wang, S.; Huang, K.; Yin, L. C.; Li, F.; Cheng, H. M. A Graphene-Pure-Sulfur Sandwich Structure for Ultrafast, Long-Life Lithium–Sulfur Batteries. *Adv. Mater.* **2014**, *26*, 625–631.
33. Chung, S. H.; Manthiram, A. A Natural Carbonized Leaf as Polysulfide Diffusion Inhibitor for High-Performance Lithium–Sulfur Battery Cells. *ChemSusChem* **2014**, *7*, 1655–1661.
34. Chung, S. H.; Manthiram, A. A Polyethylene Glycol-Supported Microporous Carbon Coating as a Polysulfide Trap for Utilizing Pure Sulfur Cathodes in Lithium–Sulfur Batteries. *Adv. Mater.* **2014**, *26*, 7352–7357.
35. Wang, X. F.; Wang, Z. X.; Chen, L. Q. Reduced Graphene Oxide Film as a Shuttle-Inhibiting Interlayer in a Lithium–Sulfur Battery. *J. Power Sources* **2013**, *242*, 65–69.
36. Arora, P.; Zhang, Z. M. Battery Separators. *Chem. Rev.* **2004**, *104*, 4419–4462.
37. Vizintin, A.; Patel, M. U. M.; Genorio, B.; Dominko, R. Effective Separation of Lithium Anode and Sulfur Cathode in Lithium–Sulfur Batteries. *ChemElectroChem* **2014**, *1*, 1040–1045.
38. Yao, H.; Yan, K.; Li, W.; Zheng, G.; Kong, D.; Seh, Z. W.; Narasimhan, V. K.; Liang, Z.; Cui, Y. Improved Lithium–Sulfur Batteries with a Conductive Coating on the Separator To Prevent the Accumulation of Inactive S-Related Species at the Cathode–Separator Interface. *Energy Environ. Sci.* **2014**, *7*, 3381–3390.
39. Bucur, C. B.; Muldoon, J.; Lita, A.; Schlenoff, J. B.; Ghostine, R. A.; Dietz, S.; Allred, G. Ultrathin Tunable Ion Conducting Nanomembranes for Encapsulation of Sulfur Cathodes. *Energy Environ. Sci.* **2013**, *6*, 3286–3290.
40. Liu, Y. B.; Cai, Z. J.; Tan, L.; Li, L. Ion Exchange Membranes as Electrolyte for High Performance Li-Ion Batteries. *Energy Environ. Sci.* **2012**, *5*, 9007–9013.
41. Huang, J. Q.; Zhang, Q.; Peng, H. J.; Liu, X. Y.; Qian, W. Z.; Wei, F. Ionic Shield for Polysulfides towards Highly-Stable Lithium–Sulfur Batteries. *Energy Environ. Sci.* **2014**, *7*, 347–353.
42. Bauer, I.; Kohl, M.; Althues, H.; Kaskel, S. Shuttle Suppression in Room Temperature Sodium–Sulfur Batteries Using Ion Selective Polymer Membranes. *Chem. Commun.* **2014**, *50*, 3208–3210.
43. Bauer, I.; Thieme, S.; Bruckner, J.; Althues, H.; Kaskel, S. Reduced Polysulfide Shuttle in Lithium–Sulfur Batteries Using Nafion-Based Separators. *J. Power Sources* **2014**, *251*, 417–422.
44. Eda, G.; Chhowalla, M. Chemically Derived Graphene Oxide: Towards Large-Area Thin-Film Electronics and Optoelectronics. *Adv. Mater.* **2010**, *22*, 2392–2415.
45. Dreyer, D. R.; Park, S.; Bielawski, C. W.; Ruoff, R. S. The Chemistry of Graphene Oxide. *Chem. Soc. Rev.* **2010**, *39*, 228–240.
46. Shao, J. J.; Lv, W.; Yang, Q. H. Self-Assembly of Graphene Oxide at Interfaces. *Adv. Mater.* **2014**, *26*, 5586–5612.
47. Joshi, R. K.; Carbone, P.; Wang, F. C.; Kravets, V. G.; Su, Y.; Grigorieva, I. V.; Wu, H. A.; Geim, A. K.; Nair, R. R. Precise and Ultrafast Molecular Sieving through Graphene Oxide Membranes. *Science* **2014**, *343*, 752–754.
48. Nair, R. R.; Wu, H. A.; Jayaram, P. N.; Grigorieva, I. V.; Geim, A. K. Unimpeded Permeation of Water through Helium-Leak-Tight Graphene-Based Membranes. *Science* **2012**, *335*, 442–444.
49. Gao, W.; Wu, G.; Janicke, M. T.; Cullen, D. A.; Mukundan, R.; Baldwin, J. K.; Brosha, E. L.; Galande, C.; Ajayan, P. M.; More, K. L.; Dattelbaum, A. M.; Zelenay, P. Ozonated Graphene Oxide Film as a Proton-Exchange Membrane. *Angew. Chem., Int. Ed.* **2014**, *53*, 3588–3593.
50. Sun, P. Z.; Zhu, M.; Wang, K. L.; Zhong, M. L.; Wei, J. Q.; Wu, D. H.; Xu, Z. P.; Zhu, H. W. Selective Ion Penetration of Graphene Oxide Membranes. *ACS Nano* **2013**, *7*, 428–437.
51. Sun, P. Z.; Zheng, F.; Zhu, M.; Song, Z. G.; Wang, K. L.; Zhong, M. L.; Wu, D. H.; Little, R. B.; Xu, Z. P.; Zhu, H. W. Selective Trans-membrane Transport of Alkali and Alkaline Earth Cations through Graphene Oxide Membranes Based on Cation–π Interactions. *ACS Nano* **2014**, *8*, 850–859.
52. Chen, C. M.; Yang, Q. H.; Yang, Y. G.; Lv, W.; Wen, Y. F.; Hou, P. X.; Wang, M. Z.; Cheng, H. M. Self-Assembled Free-Standing Graphite Oxide Membrane. *Adv. Mater.* **2009**, *21*, 3007–3011.
53. Mauro, V.; D'Aprano, A.; Croce, F.; Salomon, M. Direct Determination of Transference Numbers of $LiClO_4$ Solutions in Propylene Carbonate and Acetonitrile. *J. Power Sources* **2005**, *141*, 167–170.
54. Wang, J. L.; Lin, F. J.; Jia, H.; Yang, J.; Monroe, C. W.; NuLi, Y. N. Towards a Safe Lithium-Sulfur Battery with a Flame-Inhibiting Electrolyte and a Sulfur-Based Composite Cathode. *Angew. Chem., Int. Ed.* **2014**, *53*, 10099–10104.
55. Das, S. R.; Majumder, S. B.; Katiyar, R. S. Kinetic Analysis of the Li^+ Ion Intercalation Behavior of Solution Derived Nano-crystalline Lithium Manganate Thin Films. *J. Power Sources* **2005**, *139*, 261–268.
56. Wang, D.; Yu, Y.; Zhou, W.; Chen, H.; DiSalvo, F. J.; Muller, D. A.; Abruna, H. D. Infiltrating Sulfur in Hierarchical Architecture MWCNT@Meso C Core–Shell Nanocomposites for Lithium–Sulfur Batteries. *Phys. Chem. Chem. Phys.* **2013**, *15*, 9051–9057.
57. Guo, J.; Xu, Y.; Wang, C. Sulfur-Impregnated Disordered Carbon Nanotubes Cathode for Lithium–Sulfur Batteries. *Nano Lett.* **2011**, *11*, 4288–4294.
58. Mikhaylik, Y. V.; Akridge, J. R. Polysulfide Shuttle Study in the Li/S Battery System. *J. Electrochem. Soc.* **2004**, *151*, A1969–A1976.
59. Ryu, H. S.; Ahn, H. J.; Kim, K. W.; Ahn, J. H.; Lee, J. Y.; Cairns, E. J. Self-Discharge of Lithium–Sulfur Cells Using Stainless-Steel Current-Collectors. *J. Power Sources* **2005**, *140*, 365–369.
60. Gordin, M. L.; Dai, F.; Chen, S. R.; Xu, T.; Song, J. X.; Tang, D. H.; Azimi, N.; Zhang, Z. C.; Wang, D. H. Bis(2,2,2-trifluoroethyl) Ether as an Electrolyte Co-solvent for Mitigating Self-Discharge in Lithium–Sulfur Batteries. *ACS Appl. Mater. Interfaces* **2014**, *6*, 8006–8010.
61. Peng, H. J.; Huang, J. Q.; Zhao, M. Q.; Zhang, Q.; Cheng, X. B.; Liu, X. Y.; Qian, W. Z.; Wei, F. Nanoarchitectured Graphene/CNT@Porous Carbon with Extraordinary Electrical Conductivity and Interconnected Micro/Mesopores for Lithium–Sulfur Batteries. *Adv. Funct. Mater.* **2014**, *24*, 2772–2781.

62. Karim, M. R.; Hatakeyama, K.; Matsui, T.; Takehira, H.; Taniguchi, T.; Koinuma, M.; Matsumoto, Y.; Akutagawa, T.; Nakamura, T.; Noro, S.-i.; Yamada, T.; Kitagawa, H.; Hayami, S. Graphene Oxide Nanosheet with High Proton Conductivity. *J. Am. Chem. Soc.* **2013**, *135*, 8097–8100.
63. Huang, J. Q.; Zhang, Q.; Zhang, S. M.; Liu, X. F.; Zhu, W. C.; Qian, W. Z.; Wei, F. Aligned Sulfur-Coated Carbon Nanotubes with a Polyethylene Glycol Barrier at One End for Use as a High Efficiency Sulfur Cathode. *Carbon* **2013**, *58*, 99–106.